Anomalous uranium concentration in tourmaline-bearing leucogranite of Higher Himalaya, Nuranang, Tawang district, Arunachal Pradesh, North East India

Santu Patra[1,*], U. P. Sharma[2], Kamlesh Kumar[3] and D. K. Sinha[4]

[1]Atomic Minerals Directorate for Exploration and Research, Hyderabad 500 016, India
[2]Atomic Minerals Directorate for Exploration and Research, Nagpur 400 001, India
[3]House No. 171, Swami Colony, Phase 1, Akar Nagar, Katol Road, Nagpur 440 013, India
[4]Flat 511, Block Garnet (E), Rainbow Vista@Rock Garden, Moosapet, Hyderabad 500 018, India

Here we report anomalous uranium concentration in tourmaline-bearing leucogranite occurring at Nuranang, Tawang district, Arunachal Pradesh, North East India. The leucogranite occurs as concordant layers parallel to gneissic foliation, similar to the gneisses of the Palaeoproterozoic Se La Group. It is medium to coarse-grained, and is composed of quartz, potash feldspar and plagioclase as dominant minerals with variable proportions of muscovite, biotite, tourmaline and garnet. Apatite, zircon and pyrite are accessory minerals. Geochemically, the leucogranite is alkali-rich, peraluminous and highly differentiated. It is emplaced in a syn to late orogenic collision tectonic setting. Analyses of 10 granite samples collected at 500 m intervals show relatively high radioelemental concentration (U: 5–96 ppm, Th: 5–23 ppm, K: 2.23–7.72% and Th/U; 0.07–1.00, *n* = 10) compared to normal granite. Anomalous uranium concentration in the leucogranite is observed in a 200 m × 50 m area at Nuranang. Samples from this area have assayed 0.016–0.029% U_3O_8 and <0.005% ThO_2. Leachable U_3O_8 content determined in five samples varies from 81.25% to 87.50%. Preliminary studies indicate that uranium is in the adsorbed state associated with iron oxide and altered feldspar/clay. The findings of anomalous uranium concentration in tourmaline-bearing leucogranite likely open up a new target area for uranium search in the Higher Himalaya of Arunachal Pradesh.

Keywords: Geochemistry, leucogranite, mineralogy, petrology, tourmaline, uranium mineralization.

LEUCOGRANITE-related uranium deposits are mostly hosted in anatectic and strongly peraluminous granites[1]. Such granites are reported from the Black Hills, South Dakota, USA[2]; Guérande, Armorican Massif, France[3]; the higher Himalayas and other regions.

Among them, leucogranites of the Higher Himalayas are relatively large in volume and occur in the form of discontinuous patches in the 1500 km stretch between Pakistan and North East India[4]. In the Higher Himalayas several leucogranite, occurrences have been reported, such as at Jutial in Pakistan[5], Gangotri in Uttarakhand, India[6], Manaslu in Nepal[7] and Se La Pass in western Arunachal Pradesh, India[8,9]. These granite bodies provide important information about the tectonic metamorphic and magmatic processes associated with the Himalayan orogeny. They are well exposed at higher altitudes between the Main Central Thrust (MCT) in the south and the South Tibetan Detachment (STD) in the north.

This study deals with petrology, mineralogy and geochemistry of tourmaline-bearing leucogranite occurring at Nuranang, Tawang district, western Arunachal Pradesh[10] (Figure 1 *a* and *b*). Tourmaline-bearing leucogranite occurs as sill-like bodies parallel to the foliation in the Palaeoproterozoic Se La gneisses around Senge, Se La and Nuranang in Dirang–Tawang road section (Figure 2 *a*). Apophyses

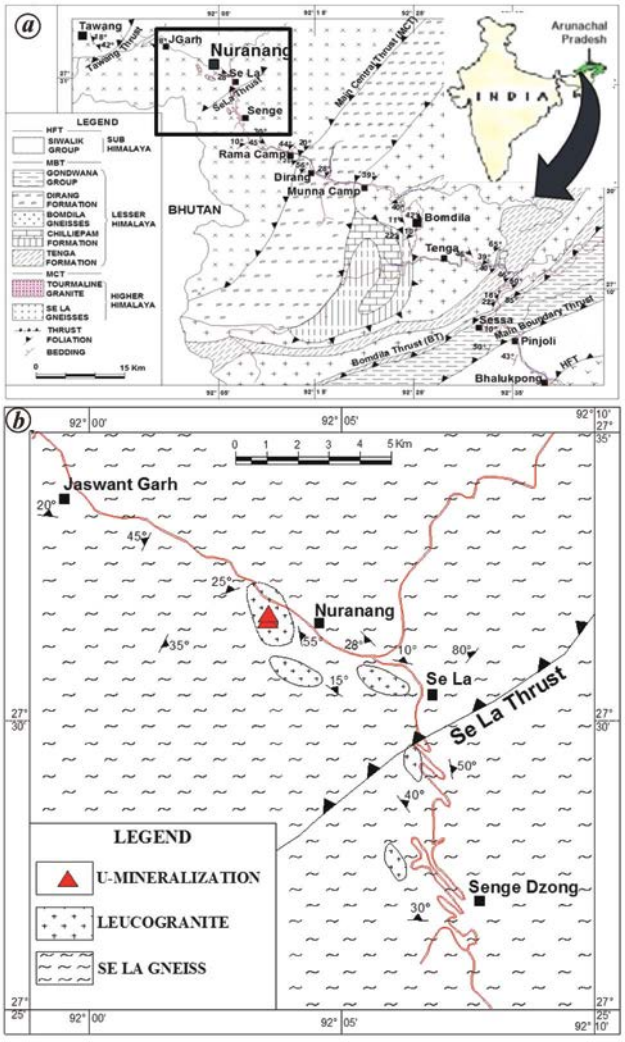

Figure 1. ***a***, Geological map of western Arunachal Pradesh, North East India showing the location of Nuranang – the study area[4]. ***b***, Geological map of the study area showing location of uranium anomaly.

*For correspondence. (e-mail: santupatra.amd@gov.in)

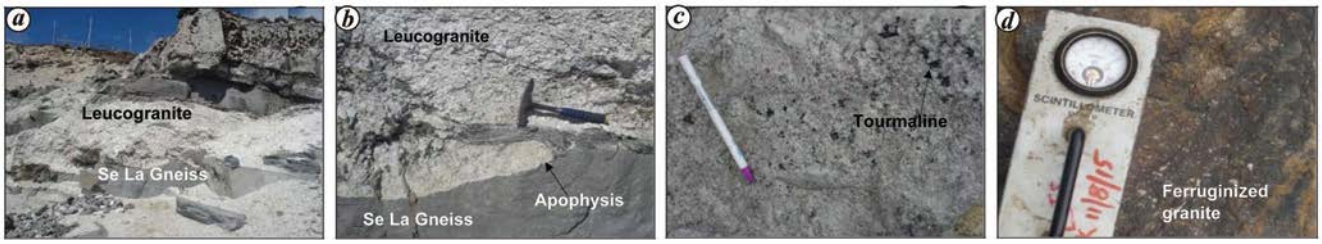

Figure 2. Field photographs: ***a***, sill of leucogranite in the Se La Gneiss; ***b***, apophysis of leucogranite in the Se La Gneiss; ***c***, tourmaline in the leucogranite; ***d***, ferruginized leucogranite showing radioactivity.

Table 1. Radiometric assay, disequilibrium factor and leachable uranium data (wt%) of leucogranite, Nuranang area, Arunachal Pradesh, North East India

Sample no.	eU_3O_8 (%)	U_3O_8 (%)	ThO_2 (%)	Ra (eU_3O_8) (%)	Leachable U (%)	Disequlibrium factor
SL/15-16/13	0.013	0.024	<0.005	0.011	87.50	2.18
SL/15-16/14	0.028	0.016	<0.005	0.026	81.25	0.62
SL/15-16/23	0.053	0.016	<0.005	0.050	87.50	0.32
NUR/16-17/07	0.011	0.019	<0.005	0.010	84.21	1.90
NUR/16-17/08	0.024	0.029	<0.005	0.023	82.75	1.26

Table 2. Modal analysis data of radioactive leucogranite, Nuranang area, Arunachal Pradesh

Sample no.	Kf	Pl	Qtz	Bt	Mu	Tour	Grt	Accessory minerals
SL/15-16/13	35.5	29.4	26.7	2.3	1.9	1.1	1.3	Ap + Zr + Op
SL/15-16/14	33.6	27.2	30.9	2	1.1	2.5	1.2	Ap + Zr
SL/15-16/23	32.9	21.6	35.4	1.3	3.7	3.1	0.5	Ap + Zr + Op
NUR/16-17/07	31.1	26.4	32.8	1.2	2	3.2	1.4	Ap + Zr
NUR/16-17/08	27.6	25.1	34.1	2.5	2.6	4.3	2.3	Ap + Zr
Average	32.14	25.94	31.98	1.86	2.26	2.84	1.34	

Kf, K-feldspar; Pl, Plagioclase; Qtz, Quartz; Bt, Biotite; Tour, Tourmaline; Grt, Garnet; Ap, Apatite; Zr, Zircon; Op, Opaques.

of leucogranite in the Se La gneisses are noticed at places (Figure 2 *b*). The tourmaline granites are medium- to coarse-grained and sometimes pegmatitic, light-coloured and tourmaline-bearing (Figure 2 *c*). Ferruginization is noticed in the uranium-mineralized, tourmaline-bearing leucogranite (Figure 2 *d*). It has been dated at 29 ± 7 Ma by Rb–Sr method with initial $^{87}Sr/^{86}Sr$ ratio of 0.7947 (ref. 11).

The anomalous uranium concentration in the tourmaline-bearing leucogranite is observed discontinuously in a 200 m × 50 m area near Nuranang. The trend of high uranium concentration zone is N30°E–S30°W. Five samples of radioactive leucogranite collected from this locality assayed 0.016–0.029% U_3O_8 and <0.005% ThO_2. Leachable U_3O_8 content varied from 81.25% to 87.50% (Table 1).

The assay results suggest disequilibrium in the uranium series in favour of both parent and daughter as U_3O_8 (β/γ)/Ra (eU_3O_8) values are greater and less than 1 respectively (DF = 0.32–2.18) (Table 1). A disequilibrium study also suggests that the uranium in the system is dynamic in nature and has been added or leached out from the system.

Petrographically, the rock is essentially a two-mica granite. Modal analysis of five radioactive granite samples of the Nuranang area (Table 2) shows that they are mainly composed of K-feldspars (32.14 in vol %), plagioclase (25.94 in vol %) and quartz (31.98 in vol %) as major minerals (Figure 3 *a* and *b*) and biotite (1.86 in vol %), muscovite (2.26 in vol %), tourmaline (2.84 in vol %) and garnet (1.34 in vol %) (Figure 3 *c*–*f*) as minor minerals. Apatite, zircon and pyrite are accessories (1.64 in vol %). As mafic minerals in this granite are <5% by volume, the rock has been classified as leucogranite and the nomenclature is consistent with earlier works in the Tibetan Plateau in similar geological setting[13]. Myrmekitic texture is observed which is represented by irregular, wormy quartz in plagioclase feldspar in contact with orthoclase feldspar (Figure 3 *b*). Muscovite occurs in association with clusters of biotite. Kinks are seen in muscovite. Garnet grains are euhedral and poikilitic with inclusions. Coarse-grained tourmaline occurs as subhedral to anhedral grains which show greenish or brownish pleochroic colours. The mineral assemblage muscovite, biotite, tourmaline and garnet indicates peraluminous and S-type nature of the granite. Usually, biotite is unaltered, but at places iron leaching from biotite flakes is observed (Figure 3 *e*). Zircon occurs as euhedral to subhedral grains either as inclusions in quartz, feldspar, muscovite and biotite (Figure 3 *e*), or along the grain boundaries of

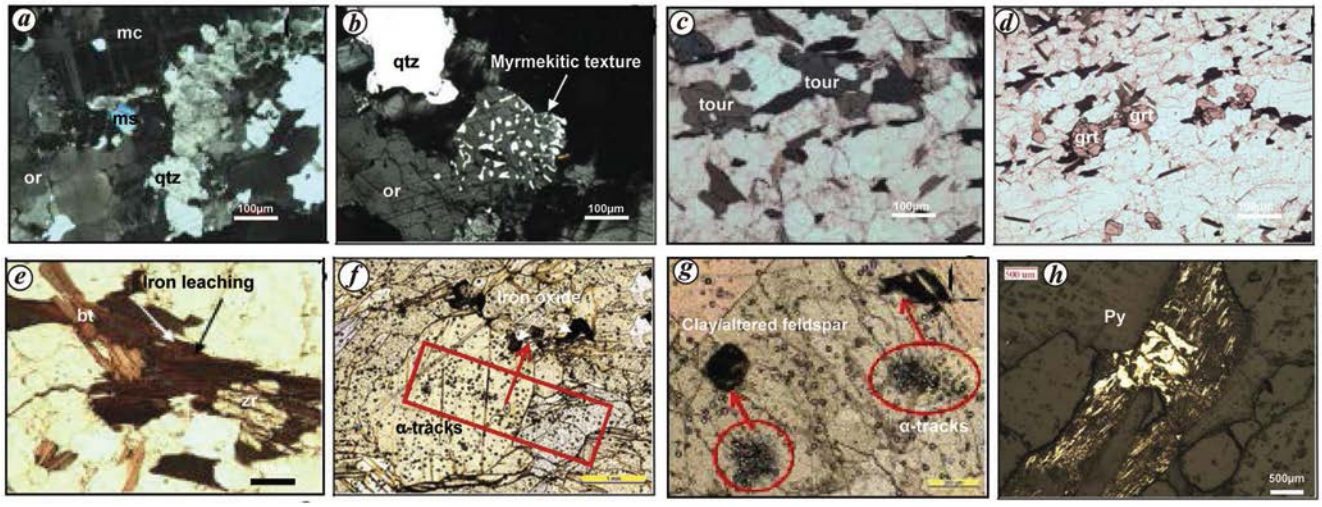

Figure 3. Photomicrographs of leucogranite showing: ***a***, quartz (qtz), microcline (mc), orthoclase (or) and muscovite (ms); ***b***, myrmekitic texture; ***c***, tourmaline (tour); ***d***, garnet (grt); ***e***, iron leaching from biotite (bt) and zircon (zr); ***f***, alpha tracks corresponding to iron oxide; ***g***, alpha tracks corresponding to clay/altered feldspar; ***h***, presence of pyrite (Py) indicating later hydrothermal activity.

Table 3. Geochemical data of leucogranite samples of Se La and Nuranang areas, Arunachal Pradesh

Sample	TG/04	TG/05	TG/07	TG/08	TG/10	TG/11	TG/12	TG/15	TG/17	TG/19
SiO_2 (%)	65.68	70.27	67.17	67.38	68.20	70.05	70.02	68.38	71.11	73.58
TiO_2 (%)	0.11	0.02	0.12	0.11	0.10	0.11	0.07	0.05	0.10	0.09
Al_2O_3 (%)	17.74	15.86	17.51	16.52	16.55	16.33	16.21	15.75	14.46	14.4
Fe_2O_3 (%)	0.37	0.03	0.16	0.16	0.09	0.16	0.37	0.25	0.29	0.37
FeO (%)	0.7	0.15	0.67	0.7	0.55	0.21	0.43	0.23	0.54	0.44
MgO (%)	0.3	<0.01	0.19	0.17	0.11	0.04	0.14	0.08	0.16	0.16
MnO (%)	0.18	0.07	0.11	0.1	0.1	0.02	0.14	0.1	0.14	0.17
CaO (%)	1.25	1.4	1.19	0.89	0.7	1.97	1.17	–	0.53	1.1
Na_2O (%)	5.16	5.41	4.35	3.93	3.92	5.24	3.6	2.49	3.15	4.45
K_2O (%)	5.33	3.66	6.84	6.89	6.94	3.21	5.33	9.3	6.15	2.69
P_2O_5 (%)	0.2	0.07	0.09	0.11	0.11	0.77	0.25	0.07	0.08	0.08
Rb (ppm)	317	146	317	306	282	155	226	439	308	156
Sr (ppm)	95	76	101	97	86	51	87	64	64	55
Ba (ppm)	502	230	440	626	803	107	288	269	303	124
U (ppm)	96	27	5	16	13	73	5	50	25	18
Th (ppm)	23	5	5	14	5	5	5	5	5	5
$Na_2O + K_2O$	10.49	9.07	11.19	10.82	10.86	8.45	8.93	11.79	9.3	7.14
K_2O/Na_2O	1.03	0.68	1.57	1.75	1.77	0.61	1.48	3.73	1.95	0.60
Fe_2O_3(t)/MgO	3.57	–	4.37	5.06	5.82	9.25	5.71	6.00	5.19	5.06
A/CNK	1.07	1.03	1.05	1.06	1.09	1.04	1.17	–	1.13	1.18
A/NK	1.24	1.23	1.20	1.19	1.19	1.35	1.39	1.11	1.22	1.41
Differential index	87.35	89.24	89.84	89.75	91.23	88.44	88.35	94.07	90.72	88.28

biotite. Low to medium density α-tracks correspond to iron oxide and clay/altered feldspar in cellulose nitrate (CN) film after 72 h exposure and treatment with nitric acid. This suggests that uranium occurs in adsorbed state with iron oxide and clays/altered feldspar (Figure 3 *f* and *g*). Pyrite is identified as an opaque mineral. It occurs along fractures, which indicates later hydrothermal activity (Figure 3 *h*).

Ten samples of tourmaline-bearing leucogranite were analysed for major and trace elements by inductively coupled plasma-optical emission spectrometry (ICP-OES), flame photometry and pellet fluorometry at the Atomic Minerals Directorate for Exploration and Research (AMD), Shillong, Meghalaya, NE India. Geochemically, the tourmaline-bearing leucogranite is characterized by moderate contents of SiO_2, Al_2O_3, Na_2O, K_2O and low contents of CaO, Fe_2O_3, FeO, MgO, MnO, TiO_2 and P_2O_5 (Table 3). The chemical composition indicates higher content of felsic minerals such as quartz, K-feldspar and plagioclase, and a lower proportion of mafic minerals. A wide variation of large-ion lithophile elements such as Rb, Sr and Ba was recorded. Samples analysed high radioelemental concentration, viz. 5–96 (av. 33) ppm of U, 5–23 (av. 8) ppm Th and 2.23–7.72% (av. 4.68%) K (Table 3). Th/U ratio varied from 0.07 to 1.00 (av.

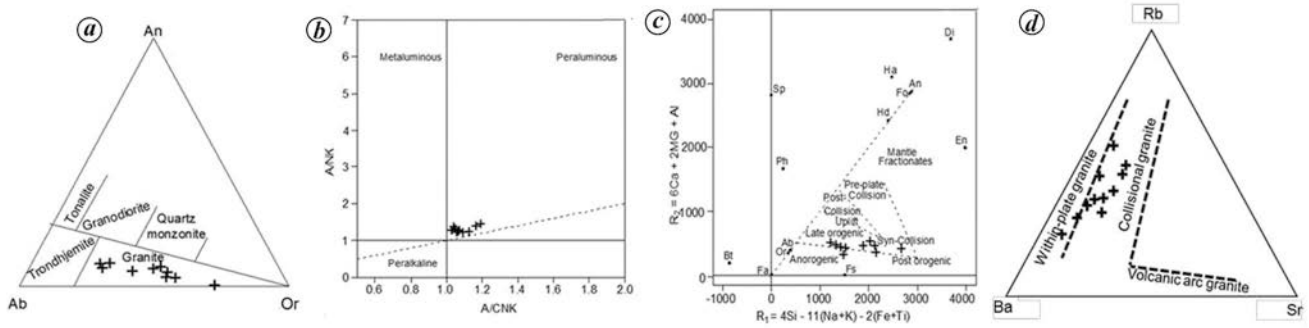

Figure 4. Geochemical plots. ***a***, Normative An–Ab–Or diagram; the samples fall in the granite field. ***b***, A/CNK versus A/NK plot showing peraluminious nature. ***c***, Tectono-magmatic discrimination diagram indicating syn-collisional to late orogenic origin. ***d***, Ba–Rb–Sr discrimination diagram showing leucogranites are collisional granites.

Table 4. Comparison of Tertiary leucogranite of Arunachal Pradesh with other Himalayan leucogranites of similar ages

Area	Jutial, Pakistan[5]	Gangotri, Uttarakhand[6]	Manaslu, Nepal Himalaya[8]	Present study Arunachal Pradesh
No. of samples (*n*)	11	40	201	10
Mineralogy	Equal proportions of quartz, oligoclase and microperthite, biotite (5–10%), muscovite (2–10%) and tourmaline with accessories zircon and apatite	Quartz, plagioclase, K-feldspar, biotite tourmaline and muscovite	Quartz (32%), subhedral zoned plagioclase ($An_{16–6}$) (37%), perthitic K feldspar (21%), muscovite (7%), biotite (3%) and tourmaline	Quartz (31.98%), K-feldspar (32.14%), plagioclase (25.94%), muscovite (2.26%), biotite (1.86%), tourmaline (2.84%), garnet (1.34%) with accessories zircon, apatite and opaques
Average composition (%)				
SiO_2	73.63	73.01	73.65	69.18
TiO_2	0.10	0.07	0.10	0.09
Al_2O_3	14.79	15.24	14.87	16.13
Fe_2O_3(t)	1.00	1.13	1.32	0.69
MnO	0.01	0.02	0.03	0.11
MgO	0.14	0.12	0.11	0.15
CaO	1.20	0.58	0.47	1.13
Na_2O	3.54	4.31	4.05	4.17
K_2O	5.16	4.56	4.56	5.63
P_2O_5	0.05	0.25	0.13	0.18
LOI	0.63	0.71	na	na
Total	100	99.65	99.29	97.48
ppm				
Rb	294	416	287	265
Ba	221	128	213	369
Sr	83	44	76	78
Th	22	4	6	8
U	20	17	9	33
Th/U	1.10	0.24	0.67	0.24
Nature of granite	High silica content (> 69% SiO_2), high alkalis (particularly K and Rb), depleted Ca and Sr, per-aluminous and S-type granite			
Initial $^{87}Sr/^{86}Sr$ ratio	0.88–0.89	0.76–0.78	0.73–0.76	0.79
Age	10–5.3 Ma (Th–Pb monazite)[18]	21.9 ± 0.5 Ma (Th–Pb monazite)[19]	22.3 ± 0.5 Ma (ionprobe monazite)[20]	29 ± 7 Ma (Rb–Sr method)[11]

0.43). Average concentration of uranium in leucogranite of the study area was eight times more than the general abundance of uranium in granite, which is 4 ppm (ref. 13). Th/U ratio (3.8–4.0) suggests enrichment of uranium in the leucogranite[14].

On normative An–Ab–Or diagram[15], samples plot in the granite field (Figure 4 *a*). Mineralogical composition as well as A/CNK versus A/NK plot indicate per-aluminous and S-type nature[16] (Figure 4 *b*). Total alkali content is high, and K_2O is more than Na_2O in most samples. CaO content in the rock is much lower than the total alkali. Higher differentiation index along with high total alkali and Fe_2O_3(t)/MgO ratio suggests the differentiated nature of the leucogranite. High K/Rb ratio indicates the presence of potassium

at the time of formation of leucogranite, and high Rb/Sr ratio suggests an upper continental crustal source for the leucogranite (Table 3). The tectono-magmatic discrimination diagram indicates that it is a syn-collisional to late orogenic granite[17] (Figure 4 *c*). The Ba–Rb–Sr discrimination diagram also indicates that it is a collisional granite[18] (Figure 4 *c*). The leucogranite is related to the collision between the Indian and Tibetan plates as evidenced by the Tertiary age.

Comparison with other leucogranites of the Higher Himalayas shows their similarity in mineralogy and geochemistry. All these leucogranites are tourmaline-bearing two-mica granites. Geochemically, these are characterized by high silica content (>69% SiO_2), high alkalis, depleted Ca, Mg and Mn, high Rb/Sr ratio, per-aluminous nature, similar age[11,19–21] and high initial $^{87}Sr/^{86}Sr$ ratios (Table 4). All these characteristics can be related to the melting of a sedimentary protolith. Radioelemental (U and Th) concentration is higher in the leucogranites of the Higher Himalaya than in normal granites, while radioelemental concentration in the granites of the study area is much higher (Table 4).

The preliminary data collected on the tourmaline-bearing leucogranites of the Higher Himalayas in a part of Arunachal Pradesh appear to be encouraging from the point of view of uranium mineralization and exploration.

1. Friedrich, M. H., Cuney, M. and Poty, B., Uranium geochemistry in peraluminous leucogranites. In *Concentration Mechanisms of Uranium in Geological Environments – A Conference Report* (eds Poty, B. and Pagel, M.), International Atomic Energy Agency, 1987, vol. 3, pp. 353–385.
2. Nabelek, P. I. and Liu, M., Petrologic and thermal constraints on the origin of leucogranites in collisional orogens. *Trans. R. Soc. Edinburgh: Earth Sci.*, 2004, **95**, 73–85.
3. Ballouard, C., Boulvais, P., Poujol, M., Gapais, D., Yamato, P., Tartèse, R. and Cuney, M., Tectonic record, magmatic history and hydrothermal alteration in the Hercynian Guérande leucogranite, Armorican Massif, France. *Lithos*, 2015, **220–223**, 1–22.
4. Islam, R., Ahmad, T. and Khanna, P. P., An overview on the granitoids of the NW Himalaya. *Him. Geol.*, 2005, **26**(1), 49–60.
5. Butler, R. W. H. *et al*., Geology of the northern part of the Nanga Parbat massif, northern Pakistan, and its implications for Himalayan tectonics. *J. Geol. Soc. London*, 1992, **149**, 557–567.
6. Scaillet, P., France-Lanord, C. and Le Fort, P., Bradinath–Gangotri plutons (Garhwal, India): petrological and geochemical evidence for fractionation processes in a High Himalayan leucogranite. *J. Volcanol. Geotherm. Res*., 1990, **44**(1–2), 163–188.
7. Le Fort, P. *et al*., Crustal generation of the Himalayan leucogranites. *Tectonophysics*, 1987, **134**, 39–57.
8. Bhattacharjee, S. and Nandy, S., Geology of the western Arunachal Himalaya in parts of Tawang and West Kameng districts, Arunachal Pradesh. *J. Geol. Soc. Ind.*, 2007, **72**, 199–207.
9. Bikramaditya Singh, R. K. and Krishnakanta Singh, A., Microstructural and geochemical studies of Higher Himalayan leucogranite: implications for geodynamic evolution of Tertiary leucogranite in the Eastern Himalaya. *Geol. J*., 2014, **49**, 28–51.
10. Bhushan, S. K., Bindal, C. M. and Aggarwal, R. K., Geology of Bomdila Group in Arunachal Pradesh. *Him. Geol*., 1991, **2**, 207–214.
11. Bhalla, J. K., Bishui, P. K. and Mathur, A. K., Geochronology and geochemistry of some granitoids of Kameng and Subansiri districts, Arunachal Pradesh. *Indian Miner*., 1994, **48**, 61–76.
12. He, X., Tan, S., Zhou, J., Liu, Z., Zhao, Z., Yang, S. and Zhang, Y., Identifying the leucogranites in the Ailaoshan–Red River shear zone: constraints on the timing of the southeastward expansion of the Tibetan Plateau. *Geosci. Front*., 2020, **11**, 765–781.
13. Rogers, J. J. W. and Adams, J. A. S., In Uranium abundances in common igneous rocks. In *Handbook of Geochemistry* (ed. Wedepohl, K. H.), Springer-Verlag, Berlin, 1969, 92-E-1–92-E-8.
14. Taylor, S. R. and McLennan, S. M., *The Continental Crust: Its Composition and Evolution*, Blackwell, Oxford, UK, 1985, p. 312.
15. O'Connor, J. T., A classification for quartz-rich igneous rocks based on feldspar ratios. United State Geological Survey, 1965, pp. 79–84.
16. Shand, S. J., *Eruptive Rocks. Their Genesis, Composition, Classification and their Relation to Ore-Deposits with a Chapter on Meteorite*, John Wiley, New York, USA, 1943.
17. De La Roche, H., Leterrier, J., Grandclaude, P. and Marchal, M., A classification of volcanic and plutonic rocks using R1–R2 diagram and major element analyses – its relationships with current nomenclature. *Chem. Geol*., 1980, **29**, 183–210.
18. El Bouseily, A. M. and El Sokkary, A. A., The relation between Rb, Ba and Sr in granitic rocks. *Chem. Geol*., 1975, **16**, 207–219.
19. Schneider, D. A., Zeitler, P. K., Edwards, M. A. and Kidd, W. S. F., Geochronological constraints on the geometry and timing of anatexis and exhumation at Nanga Parbat: a progress report. *EOS*, 1997, **237**, 312.
20. Harrison, T. M., Lovera, O. M. and Groove, M., New insights into the origin of two contrasting Himalayan granite belts. *Geol.*, 1997, **25**, 899–902.
21. Harrison, T. M. and McKeegan, K. D., $^{208}Pb/^{232}Th$ ion microprobe dating of monazite and Himalayan Tectonics. *Geol. Soc. Am. Abstr*., 1994, **26**, A-367.

ACKNOWLEDGEMENTS. We thank the scientific officers and staff of the Physics, Chemistry and Petrology Laboratories, Atomic Minerals Directorate for Exploration and Research, North Eastern Region, Shillong for analytical support.

Received 2 April 2022; re-revised accepted 1 December 2022

doi: 10.18520/cs/v124/i2/253-257

Nutritional value of representative termite species with an emphasis on *Odontotermes obesus* (Rambur)

M. Ranjith, C. M. Kalleshwaraswamy*, Sharanabasappa S. Deshmukh and G. A. Kavya Yadav

Department of Entomology, College of Agriculture, Keladi Shivappa Nayaka University of Agricultural and Horticultural Sciences, Navile, Shivamogga 577 204, India

Dewinged termite imagoes are considered to be delicious human food around the world. The nutrient composition may vary with respect to the species. In the present study, imagoes of three termite species, viz. *Odontotermes obesus*, *Coptotermes heimi* and *Microtermes obesi* were used to compare their protein composition. Additionally, the commonest species, *O. obesus* was used for

*For correspondence. (e-mail: kalleshwaraswamycm@uahs.edu.in)